Synthesis, Hydration Properties and Environmentally Friendly Features of Calcium Sulfoaluminate Cements

G. L. Valenti[1], M. Marroccoli[1], F. Montagnaro[2], M. Nobili[1], A. Telesca[1],
[1]*University of Basilicata, Potenza, Italy*
[2]*University of Naples "Federico II", Naples, Italy*

1. INTRODUCTION

In particular applications special cements, obtained from non-Portland clinkers, behave better than Portland and blended cements, but their peculiar composition can also be exploited to give to their manufacturing process a more pronounced environmentally friendly character [1-11]. In this regard important features are:

1) synthesis temperatures lower than those requested (1450°-1500°C) by ordinary Portland cement (OPC) clinkers;
2) clinkers easier to grind;
3) reduced amount of limestone in the kiln raw mix and, consequently, reduced thermal input and CO2 generation;
4) greater usability of industrial wastes and by-products whose reuse and disposal is quite complicated.

All these features are shown by calcium sulfoaluminate (CSA) cements, mainly composed by $C_4A_3\bar{S}$, C_2S, $C_5S_2\bar{S}$ and a variety of calcium aluminates (C_3A, CA, $C_{12}A_7$, C_4AF, C_2AS and CAS_2) as well as lime and/or calcium sulfate (depending on the type of application). As a matter of fact, the temperatures needed to obtain $C_4A_3\bar{S}$, the key-component of CSA cements, are about 150°-200°C lower than those required by OPC clinkers which are furthermore less porous and more difficult to grind, due to the considerable amount of liquid phase formed at the maximum synthesis temperature. The specific CaO requirement (referred to the unit mass of compound) for $C_4A_3\bar{S}$ is 0.367, namely 50%, 56%, 59% and 80% of that necessary for C_3S, C_2S, C_3A and C_4AF, respectively. Hence, during the manufacture of CSA cements, a reduced limestone concentration in the raw mix is needed and a related remarkable decrease of the heat requirement is achieved, considering that limestone calcination mostly accounts for the kiln thermal balance. Correspondingly, the CO_2 emission deriving from the raw materials decomposition is also reduced. The specific carbon dioxide generation, in terms of CO_2/pure cement compound mass ratio, is for $C_4A_3\bar{S}$ 0.216 against 0.578,0.511, 0.489 and 0.362 for C_3S, C_2S, C_3A and C_4AF, respectively [11].

Regarding the use of industrial wastes and by-products for CSA cement manufacture, fluidized bed combustion (FBC) waste is worthy of consideration [10]. It is mainly composed by CaO, SiO_2, Al_2O_3 and SO_3 deriving from coal ash and exhausted sulfur sorbent. Its utilization in ordinary cement and concrete industries is made difficult by the

exothermal and expansive phenomena occurring during the hydration, which complicate also the landfill disposal.
FBC waste has a relatively low Al_2O_3 content and its use in the raw mix generating CSA clinker requires additional sources of alumina. In order to achieve a significant saving of an expensive natural material like bauxite, cheap sources of Al_2O_3, such as red mud or low-quality pulverized coal fly ash, can be utilized.
With reference to the various CSA formulations, those characterized by rapid hardening and dimensional stability are very interesting not only for their technical behaviour, but also from the environmental point of view. As a matter of fact, these cements are generally produced adding to CSA clinker significant amounts of calcium sulfate. To this end, large quantities of chemical gypsums, whose landfill disposal is made difficult by their water solubility, can be used. Among chemical gypsums, flue gas desulfurization (FGD) gypsum, which is being produced worldwide in increasing amounts within coal- and oil- fired electric power plants, is worthy of consideration.
This paper is aimed at evaluating on laboratory scale the suitability of FBC waste, pulverized coal fly ash, red mud and FGD gypsum as raw mix components for the manufacture of CSA clinkers. Furthermore, two laboratory-made high performance cements consisting of CSA clinker and FGD gypsum were paste hydrated and investigated by XRD, DTA-TGA and SEM analyses as well as mercury porosimetry.

2. EXPERIMENTAL

2.1 Materials

As sources of raw materials, AR chemicals (calcium carbonate and aluminium oxides), natural materials (limestone and bauxite) and industrial wastes such as FBC waste (available in two streams, fly and bottom ash), pulverized coal fly ash (FA), red mud and FGD gypsum were used. The chemical composition of natural materials and industrial wastes is indicated in Table 1.

2.2 Testing procedures

Nine mixtures (M1÷M9), having the composition shown in Table 2, were prepared. M1, M2, M3, M4 and M5 contained $CaCO_3$ and FBC fly ash. M1 and M2 were ternary mixes consisting also of Al_2O_3 or bauxite, respectively. Both bauxite and red mud were used as sources of alumina in mixtures M3, M4 and M5. FA, FGD gypsum, bauxite, FBC fly ash and limestone were the components of M6 and M7. M8 and M9 contained FA, bauxite, FBC waste (consisting of both fly- and bottom-ash) and limestone; M9 contained also FGD gypsum. All the mixtures were heated in a laboratory electric oven for 2 hours in the temperature range 1150°÷1300°C, then submitted to X-ray diffraction (performed by a PHILIPS PW1710 apparatus operating between 5° and 60° 2θ, Cu $K\alpha$ radiation) in order to evaluate both conversion and selectivity of the reacting systems.

Table 1: Chemical composition of natural materials and industrial

wastes, mass %.

	limestone	bauxite	FBC fly ash	FBC bottom ash	FA	red mud	FGD gypsum
CaO	54.70	1.69	24.20	43.12	4.30	6.07	32.04
SO_3	-	0.03	12.80	25.89	0.04	5.60	45.77
Al_2O_3	-	55.22	13.71	5.85	22.80	24.60	0.08
SiO_2	-	6.48	23.23	18.45	35.08	15.40	0.10
MgO	0.30	-	1.04	1.00	1.13	0.46	0.37
SrO	-	0.03	-	-	0.11	-	-
P_2O_5	-	0.01	-	-	0.10	-	-
TiO_2	-	2.34	0.82	0.48	1.52	5.81	-
Fe_2O_3	-	6.25	6.74	3.15	8.20	14.50	-
Mn_3O_4	-	-	0.07	0.08	0.10	0.02	-
Na_2O	-	-	-	-	-	12.10	0.03
l.o.i.*	42.61	27.68	16.26	1.39	25.85	9.96	20.59
Total	97.61	99.73	98.87	99.41	99.23	94.52	98.98

** loss on ignition, according to EN 196 Standard*

Table 2: Composition of raw mixtures, mass %.

Mixture	M1	M2	M3	M4	M5	M6	M7	M8	M9
$CaCO_3$ AR	41.40	40.30	42.00	40.00	35.00	-	-	-	-
Al_2O_3 AR	16.30	-	-	-	-	-	-	-	-
FA	-	-	-	-	-	13.97	19.43	11.63	23.52
FGD gypsum	-	-	-	-	-	4.27	6.28	-	6.05
bauxite	-	24.50	13.00	15.00	20.00	17.65	17.06	18.23	16.22
red mud	-	-	16.00	10.00	10.00				
FBC fly and bottom ash*	-	-	-	-	-	-	-	21.61	10.08
FBC fly ash	42.30	35.20	29.00	35.00	35.00	17.08	10.46	-	-
limestone	-	-	-	-	-	47.03	46.77	48.53	44.13

** fly/bottom mass ratio equal to 1.5*

Table 3 shows the potential concentration values of $C_4A_3\bar{S}$ and C_2S in the burning products of the nine mixtures. They were calculated assuming that SO_3 and Al_2O_3 on the one hand, and SiO_2, on the other, react to give only $C_4A_3\bar{S}$ and C_2S, respectively; furthermore, solid solution effects were neglected.

Table 3: Potential concentration of $C_4A_3\bar{S}$ and C_2S in the burning

products of raw mixtures, mass %.

Mixture	M1	M2	M3	M4	M5	M6	M7	M8	M9
$C_4A_3\bar{S}$	52.50	49.70	41.70	43.16	42.70	39.54	41.61	38.01	41.30
C_2S	34.80	39.90	40.10	34.30	33.10	43.07	43.70	45.53	39.43
$C_4A_3\bar{S}$ + C_2S	87.30	89.60	81.80	77.46	75.80	82.61	85.31	83.54	80.73

For the hydration tests, two CSA cements, CEM1 and CEM2, were prepared by grinding the clinkers obtained from M7 and M8 respectively, with 15.0% and 13.7% gypsum, in the order. The FGD gypsum contents were the stoichiometric amounts required by the following reaction:

$$C_4A_3\bar{S} + 2C\bar{S} + 38H \Rightarrow C_6A\bar{S}_3H_{32} + 2AH_3$$

Cement samples were paste hydrated (water/cement mass ratio, 0.50) and investigated by XRD, DTA-TGA and SEM analyses as well as mercury porosimetry. The pastes, shaped as cylindrical discs (15 mm high, 30 mm in diameter), were cured in a FALC WBMD24 thermostatic bath at 20°C for times ranging from 3 hours to 28 days. At the end of each aging period, the discs were in part submitted to mercury porosimetry, in part broken for SEM observations or pulverized for XRD and DTA-TGA analyses after grinding under acetone (to stop hydration), followed by treating with diethyl–ether (to remove water) and storing in a desiccator over silica gel-soda lime (to ensure protection against H_2O and CO_2).

DTA-TGA was carried out through a NETZSCH TASC 414/3 apparatus, operating between 20° and 1000°C with a heating rate of 10°C/min.

For SEM observations a PHILIPS XL-30 ESEM instrument was used. Specimens were metallized with gold by means of an EMITECH K 950 apparatus.

Porosity measurements were performed with a THERMO FINNIGAN PASCAL 240 Series porosimeter (maximum pressure, 200 MPa; resolution 0.01 MPa up to 100 MPa and 0.1 MPa up to 200 MPa) equipped with a low-pressure unit (140 Series) able to generate a high vacuum level (10 Pa) and operate between 100 and 400 kPa.

3. RESULTS AND DISCUSSION

3.1 Synthesis of CSA cements

From the examination of the XRD data concerning all the burning products of Mixture M1, it can be argued that: a) $C_4A_3\bar{S}$ and C_2S are the main components; b) minor phases are present at every synthesis temperature (unreacted CaO and $CaSO_4$ at 1100° and 1150°C; CA at 1150° and 1200°C; $C_5S_2\bar{S}$ and C_2AS at 1250°C). For $C_4A_3\bar{S}$ the

optimum conversion temperature was 1250°C (Fig.1); for C_2S it was about 1150°C (Fig. 2).

For the burning products of Mixture M2, the presence of $C_4A_3\overline{S}$ and C_2S as main components and the occurrence of minor phases were also observed. The optimum conversion temperatures for both $C_4A_3\overline{S}$ (Fig.1) and C_2S (Fig.2) was about 1200°C. The selectivity towards these phases is lower for Mixture M2 due to the greater number and the higher content of secondary phases related to the contribution of oxides, different from Al_2O_3, given by bauxite. At 1150°C, unreacted calcium sulfate and lime were present together with $C_5S_2\overline{S}$ and C_2AS. At higher temperatures it has been found: a) the disappearance of calcium sulfate (since1200°C); b) the disappearance of lime (since 1250°C); c) the persistence of $C_5S_2\overline{S}$ and C_2AS; d) the appearance of C_3A (since 1200°C).

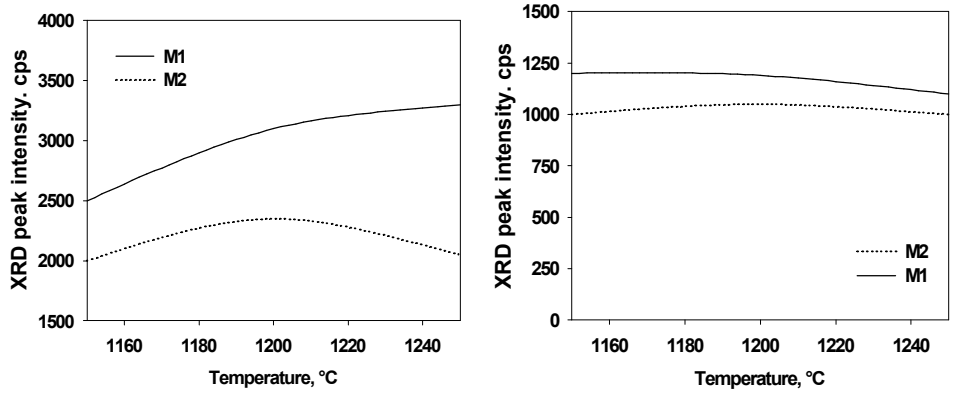

Fig. 1 (left): $C_4A_3\overline{S}$-XRD intensity (main peak, counts per second) for the burning products of mixtures M1 (continuous curve) and M2 (dotted curve) vs. synthesis temperature.

Fig. 2 (right): C_2S-XRD intensity (main peak, counts per second) for the burning products of mixtures M1 (continuous curve) and M2 (dotted curve) vs. synthesis temperature.

The data concerning the burning products of the mixtures M3, M4, M5 heated at 1100° and 1200°C (Table 4), showed that the phases different from $C_4A_3\overline{S}$ and C_2S play a more significant role.

For M5, the main component was C_2AS; for M3 and M4 there was a considerable presence of secondary phases like C_2AS, $C_{12}A_7$, C_3A and calcium sulfate together with $C_4A_3\overline{S}$ and C_2S which were however the main components. Hence the combined use of bauxite and red mud resulted in a further decrease of the amount of the expected hydraulic phases.

Table 4: Qualitative composition of the burning products at 1100° and 1200°C of raw mixtures containing bauxite and red mud –XRD data (symbols indicate peak intensities +++=high, ++=medium, +=low).

T=1100°C	mixtures		
phase	M3	M4	M5
$C_4A_3\bar{S}$	+++	+++	++
C_2S	+++	+++	++
C_2AS	++	++	+++
C_3A	+	+	-
$C_{12}A_7$	++	++	-
$C\bar{S}$	++	++	-
T=1200°C	mixtures		
phase	M3	M4	M5
$C_4A_3\bar{S}$	+++	+++	++
C_2S	+++	+++	++
C_2AS	+	+	+++
C_3A	++	++	-
$C_{12}A_7$	+	+	-
$C\bar{S}$	+	+	-

As far as mixtures M6, M7, M8 and M9 are concerned, $C_4A_3\bar{S}$ and C_2S were again, in the order, the main mineralogical phases. Reactants were absent in the burning products of M6, M7 and M9 while M8, upon heating at all the temperatures investigated, showed the presence of a little amount of $CaSO_4$. Secondary phases were completely absent in M6 and M9 burnt at 1200°C; upon heating at 1250°C and 1300°C, M6 and M9 revealed the presence, in low concentrations, of brownmillerite, C_4AF, and calcium sulfosilicate, $C_5S_2\bar{S}$, respectively. For M7 and M8, at every heating temperature, respectively weak peaks of $C_5S_2\bar{S}$ and C_4AF were found. Figs.3-4 and Figs. 5-6 indicate, for mixtures M6-M7 and M8-M9, respectively, the XRD peak intensities of $C_4A_3\bar{S}$ and C_2S as a function of the burning temperature. It was generally observed a significant influence of the synthesis temperature on the $C_4A_3\bar{S}$ and C_2S concentrations. However the optimum temperature for obtaining the maximum amount of $C_4A_3\bar{S}$ was about 1250°C for M6 and M8, 1200°C for M7 and 1300°C for M9. As far as C_2S is concerned, the optimum temperature was 1300°C for M6 and 1200°C for M7, M8 and M9.

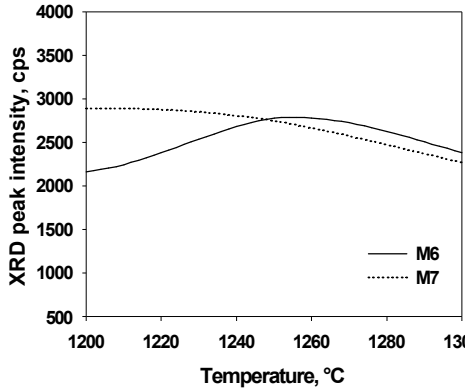

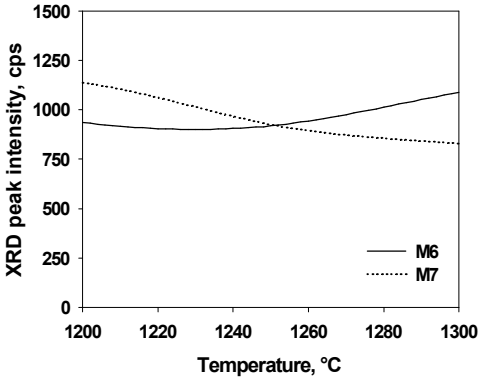

Fig. 3 (left): $C_4A_3\bar{S}$-XRD intensity (main peak, counts per second) for the burning products of mixtures M6 (continuous curve) and M7 (dotted curve) vs. synthesis temperature.

Fig. 4 (right): C_2S-XRD intensity (main peak, counts per second) for the burning products of mixtures M6 (continuous curve) and M7 (pink curve) vs. synthesis temperature.

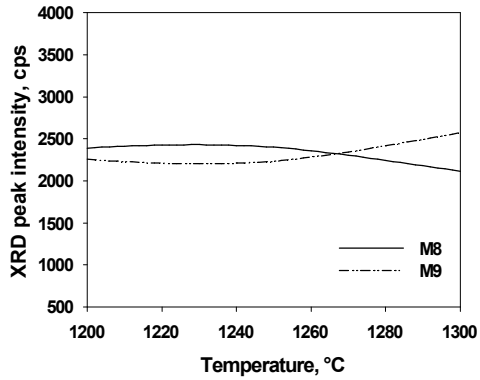

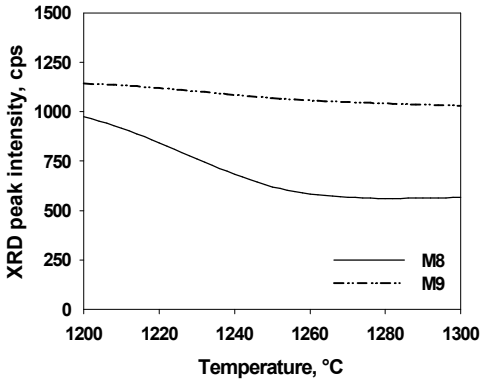

Fig. 5 (left): $C_4A_3\bar{S}$-XRD intensity (main peak, counts per second) for the burning products of mixtures M8 (continuous curve) and M9 (dotted curve) vs. synthesis temperature.

Fig. 6 (right): C_2S-XRD intensity (main peak, counts per second) for the burning products of mixtures M8 (continuous curve) and M9 (dotted curve) vs. synthesis temperature.

3.2 Hydration properties of CSA cements

The hydration properties of both CSA cements, evaluated by means of XRD, DTA-TGA, SEM and mercury porosimetry, were very similar. Hereafter, only the results obtained with CEM 2 are reported.

3.2.1 XRD results

Figs.7 and 8 show the XRD patterns for the cement paste cured at 3 hours and 28 days, respectively. At the shortest aging period, ettringite forms but considerable amounts of $C_4A_3\bar{S}$ and gypsum are still

present. At 28 days these latter phases disappear and ettringite is the dominant phase. No other hydration products are observed; phase s different from $C_4A_3\bar{S}$ and gypsum such as C_2S and C_2AS do not seem involved in the hydration.

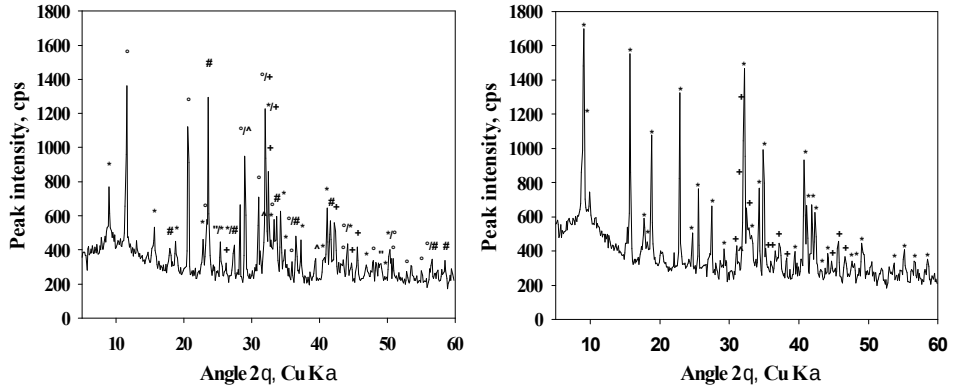

Fig.7 (left): XRD pattern of cement paste hydrated at 3h: *=ettringite #= $C_4A_3\bar{S}$, °= $C\bar{S}H_2$, +=β-C_2S, "=$CaSO_4$, ^=C_2AS

Fig.8 (right): XRD pattern of cement paste hydrated at 28d: *=ettringite +=β-C_2S, ^=C_2AS

3.2.2 DTA-TGA results

Fig.9 shows the DTA-TGA thermograms for the same samples submitted to XRD analysis. At 3 hours of aging, the effects related to the presence of ettringite and gypsum are clearly evident (DTA endothermal peaks at about 159°C and 170°-185°C, respectively). The presence of $Al(OH)_3$ in a little amount is also observed (DTA endothermal peak at 285°C).

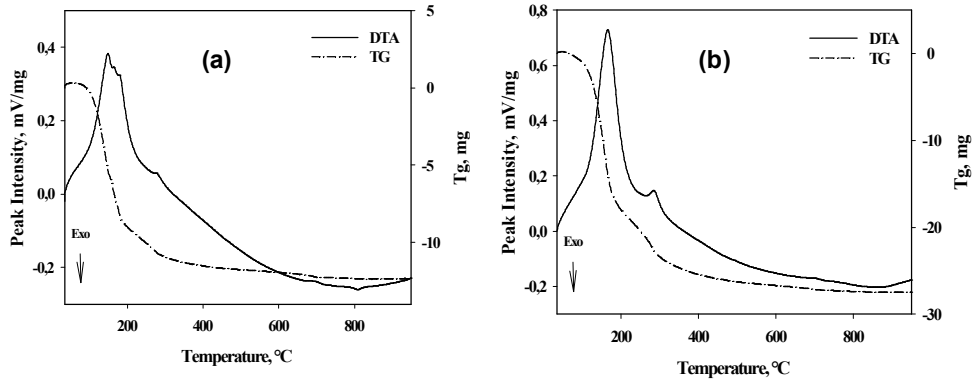

Fig.9: DTA-TGA thermograms for CSA cement paste cured at: (a) 3h; (b) 28d.

At 28 days of curing, only the ettringite and $Al(OH)_3$ signals, increased in intensity, were detected.

3.2.3 SEM observations

Fig. 10 shows micrographs of CSA cement pastes cured at early ages, when the clearest images were obtained. At 3 hours, Figs.10 (a), the ettringite particles appear on the surfaces of the anhydrous grains. At 16 hours, Figs.10 (b), the growth of the characteristic ettringite prismatic crystals, having an hexagonal cross section, is particularly evident.

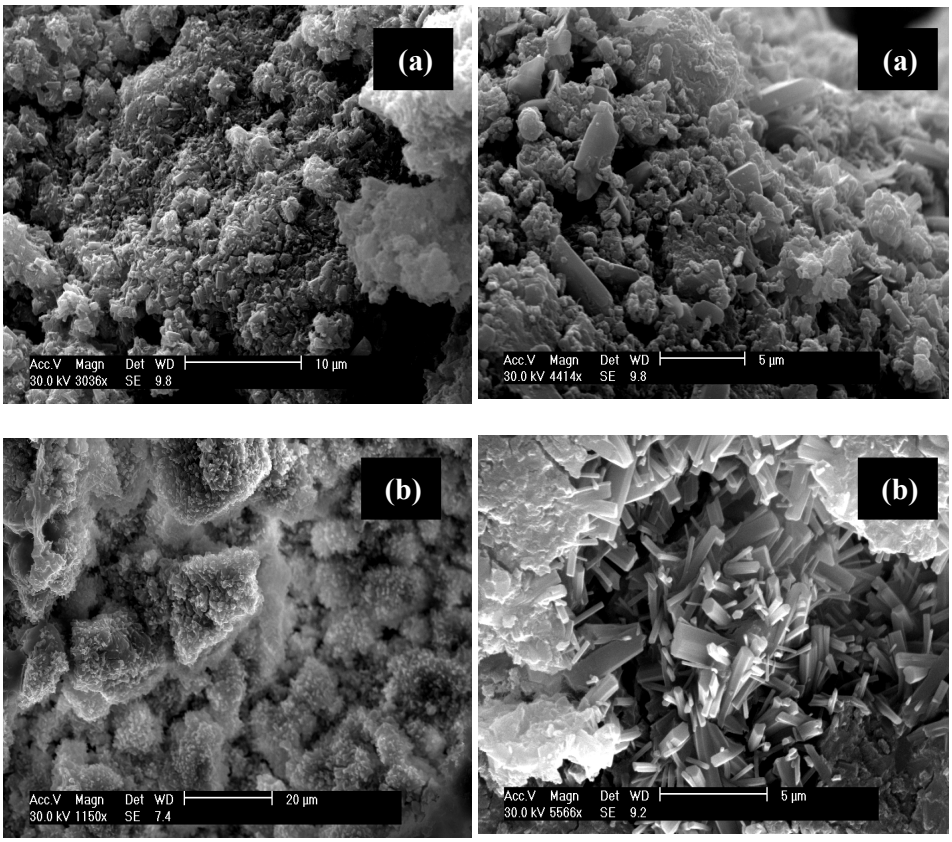

Fig.10: SEM (SE) micrographs of CSA cement pastes cured at: (a) 3h; (b) 16h (lower magnitude on the left side).

3.2.4 Porosimetric results

For each sample, two plots can be obtained from the porosimetric analysis: a) cumulative and b) derivative Hg intruded volume vs. pore radius. With increasing pressure, mercury gradually penetrates the bulk sample volume. If the pore system is composed by an interconnected network of capillary pores in communication with the outside of the sample, mercury enters at a pressure value corresponding to the smallest pore neck. If the pore system is discontinuous, mercury may penetrate the sample volume if its pressure is sufficient to break through pore walls. In any case, the pore width related to the highest rate of mercury intrusion per change in pressure is known as the “critical” or “threshold” pore width [12]. Unimodal, bimodal or multimodal distribution of pore sizes can be obtained, depending on the

occurrence of one, two or more peaks, respectively, in the derivative volume plot.
The porosimetric characteristics of CSA cement pastes cured at 6 hours, 3 and 28 days are shown in Fig.11. The pore size distribution is bimodal at 6 hours and 3 days (the first and the second threshold pore radius being included in the range 110-30 and 11-6 nanometers, respectively) and unimodal at 28 days (being the size of the threshold pore radius equal to about only 3 nanometers). The first peak, at higher porosity, is related to the lowest size of pore necks connecting a continuous system consisting of a network of capillary pores; the second peak, at lower porosity, corresponds to the pressure required to break through the blockages formed by the hydration products [13-14].

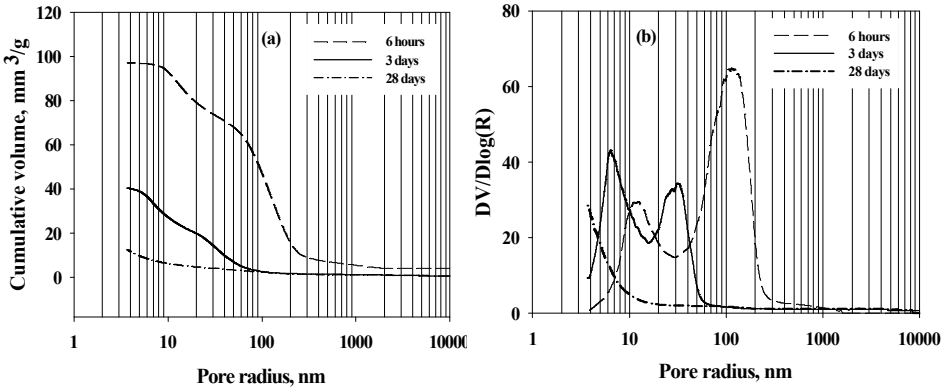

Fig.11: Intruded Hg volume vs. pore radius for CSA cement pastes cured at various ages: (a) cumulative plot; (b) derivative plot.

The hydraulic behaviour outlined by all the microstructural investigations is similar to that shown by industrial CSA cements. [14-15].

4. CONCLUSIONS

Calcium sulfoaluminate (CSA) cements not only have remarkable technical properties, but also show interesting environmentally friendly features related to their manufacturing process. CSA clinkers are easier to grind than OPC clinkers due to their porous structure associated with the lack of liquid phase at the clinkerization temperature. Moreover, higher thermal energy savings and a more pronounced environmental safeguard can be achieved owing to reduced synthesis temperature, limestone requirement and CO_2 emission. This is due to the peculiar characteristics of the main CSA cement component, $C_4A_3\bar{S}$, which has specific CaO requirement and CO_2 generation equal to 0.367 and 0.216 respectively, against 0.737 and 0.578 for C_3S, 0.651 and 0.511 for C_2S, 0.622 and 0.489 for C_3A, 0.461 and 0.362 for C_4AF.
Another noteworthy environmentally friendly feature of CSA cements is

related to the usability of industrial wastes and by-products difficult to reuse and dispose of, such as fluidized bed combustion (FBC) waste, red mud, low-quality pulverized coal fly ash and chemical gypsum.

High performance CSA cement formulations, characterized by rapid hardening and dimensional stability, are interesting from the environmental point of view because they require a significant addition of calcium sulfate, so enabling both a decrease of clinker concentration in the cement and an enhancement of chemical gypsum utilization. In particular, flue gas desulfurization (FGD) gypsum, generated worldwide in increasing amounts, can be conveniently used.

After burning in a laboratory electric oven, raw mixes, aimed at obtaining high performance CSA cements and based on FBC bottom – and/or fly-ash, calcium carbonate or limestone, alumina or bauxite, showed generally high conversion degrees of the reactants and good selectivity towards $C_4A_3\bar{S}$ and C_2S. When a cheap source of alumina (low quality pulverized coal ash, FA, or red mud) was used in order to reduce the bauxite content of the raw mix, much better results were obtained with FA. Moreover, FGD gypsum was added to generating raw mix and/or clinker. Two laboratory-made high performance cements, obtained by mixing two synthetic preparations of CSA clinker with FGD gypsum, exhibited hydration properties similar to those shown by CSA industrial cements. In particular both the fast formation of ettringite and the rapid establishment of prevailing low porosity regions were observed in the hydrated systems.

5. REFERENCES

[1]P.K. Mehta, Investigations on energy-saving cements, World Cem Technol 11 (4), 1980, 166-177.

[2] G.A. Mudbhatkal, P.S. Parmeswaran, A.S. Heble, B.V.B. Pai, A.K. Chatterjee, Non-alitic cement from calcium sulphoaluminate clinker-Optimisation for high-strength and low-temperature application, Proc 8th Int Congr Chem Cem, Rio de Janeiro, Brazil, 1986, vol. IV, pp. 364-370.

[3] J. Beretka, L. Santoro, N. Sherman, G.L. Valenti, Synthesis and properties of low energy cements based on $C_4A_3\bar{S}$, Proc. 9th Int. Congr Chem Cem, New Delhi, India, 1992, vol. III, pp.195-200.

[4] J. Beretka, B. de Vito, L. Santoro, N. Sherman, G.L. Valenti, Hydraulic behaviour of calcium sulphoaluminate-based cements derived from industrial process wastes, Cem Concr Res 23, 1993, 1205-1214.

[5] J. Majling, S. Sahu, M.Vlna, Della M. Roy, Relationship between raw mixture and mineralogical composition of sulphoaluminate belite clinkers in the system $CaO-SiO_2-Al_2O_3-Fe_2O_3-SO_3$, Cem Concr Res 23, 1993, 1351-1356.

[6] G. Belz, J. Beretka, M. Marroccoli, L. Santoro, N. Sherman, G.L. Valenti, Use of fly ash, blast furnace slag and chemical gypsum for the synthesis of calcium sulphoaluminate based cements, Proc 5th CANMET/ACI Int. Conf. on Fly Ash, Silica Fume, Slag and Natural Pozzolans in Concrete, Milwaukee, USA, 1995, SP-153, 1995, vol. 1,

pp.513-530.
[7] J. Beretka, R. Cioffi, M. Marroccoli, G.L. Valenti, Energy-saving cements obtained from chemical gypsum and other industrial wastes, Waste Management 16, 1996, 231-235.
[8] K. Ikeda, K. Fukuda, H. Shima, Calcium sulphoaluminate cements prepared from low -alumina waterworks slime, Proc. 10th Int Congr Chem Cem, Goteborg, Sweden, 1997, vol. 1, pp. 1i025 (8 pp.).
[9] P. Arjunan, M.R. Silsbee, Della M. Roy, Sulfoaluminate-belite cement from low-calcium fly ash and sulphur-rich and other industrial by-products, Cem Concr Res 29, 1999, 1305-1311.
[10] G. Bernardo, M. Marroccoli, F. Montagnaro, G.L. Valenti, Use of fluidized bed combustion wastes for the synthesis of low energy cements, Proc. 11th Int Congr Chem Cem, Durban, South Africa, 2003, vol. 3, pp. 1227-1236.
[11] E. Gartner, Industrially interesting approaches to ''low-CO_2'' cements, Cem Concr Res 34, 2004, 1489-1498.
[12] D.N. Winslow, S. Diamond, A mercury porosimetry study of the evolution of porosity in Portland cement, ASTM J. Materials 3 (1970) 564-585.
[13] R.A. Cook, K.C. Hover, Mercury porosimetry of hardened cement pastes, Cem Concr Res 29, 1999, 933-943.
[14] G. Bernardo, A. Telesca, G. L. Valenti, A porosimetric study of calcium sulfoaluminate cement pastes cured at early ages, Cem Concr Res 36, 2006, 1042-1047.
[15] M. Marroccoli, M. Nobili, A. Telesca, G. L. Valenti, Use of wastes generated within coal-fired power stations for the synthesis of calcium sulphoaluminate cements, accepted for publication on the Proceedings of the 7th International Congress "Concrete: Construction's Sustainable Option", Dundee, Scotland, 4-6 September 2007, in press.